

XII. Gaseous Detectors

For a detailed review of the physics of gaseous detectors, see J. Va'vra, *Gaseous Wire Detectors* in G. Herrera Corral and M. Sosa Aquino (eds.), *Instrumentation in Elementary Particle Physics*, AIP Conference Proceedings 422, Woodbury, NY 1998

Incident radiation forms electron-ion pairs. In gases the ionization energy is typically ~ 30 eV.

Electrons and ions drift under influence of electric field and induce signal current on detector electrodes.

a) Drift velocity of electrons

As electrons move in the gas they suffer random collisions.

The number of collisions within a distance dx

$$dn = \frac{1}{v\tau} dx$$

where v is the velocity and τ the average time between collisions.

The collision rate $1/\tau$ is proportional to the density of the gas N and the instantaneous electron velocity v'

$$\frac{1}{\tau} = N\sigma v'$$

Between collisions the electron is accelerated

$$m \frac{dv}{dt} = q_e E$$

and the electron's displacement vs. time

$$x(t) = \frac{1}{2} \frac{q_e}{m} E t^2$$

The time between collisions is determined by the probability of collisions. In an interval dt the differential probability dP is

$$dP = \frac{1}{\tau} e^{-t/\tau} dt$$

The average displacement is found by averaging $x(t)$ over time, using the collision probability

$$\langle x \rangle = \int_0^{\infty} \frac{1}{2} \frac{q_e}{m} Et^2 \frac{1}{\tau} e^{-t/\tau} dt = \frac{q_e}{m} E\tau^2$$

The average drift velocity

$$\langle v \rangle = \frac{\langle x \rangle}{\tau} = \frac{q_e}{m} E\tau \equiv \mu E$$

Since τ is inversely proportional to the density of the gas, the drift velocity

$$v \propto \frac{E}{p}$$

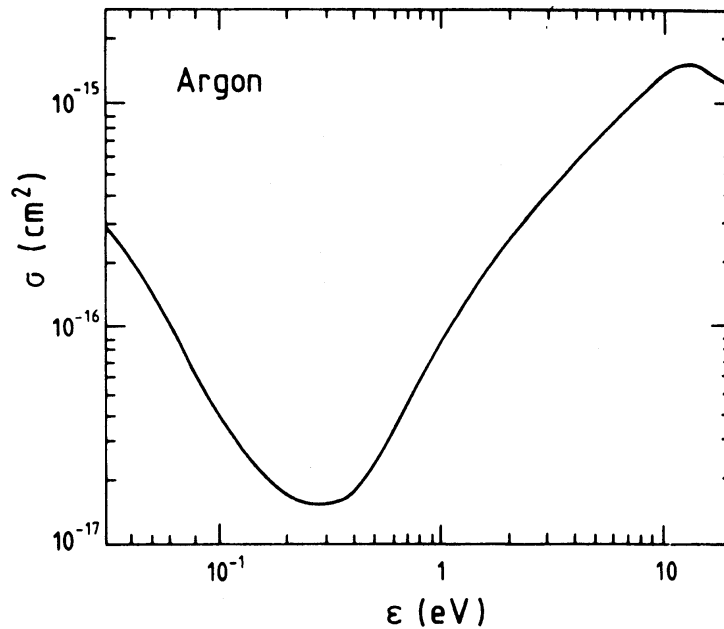
where p is the gas pressure, so the expression for the drift velocity is commonly written as

$$v = \mu E \frac{p_0}{p} = \mu p_0 \frac{E}{p}$$

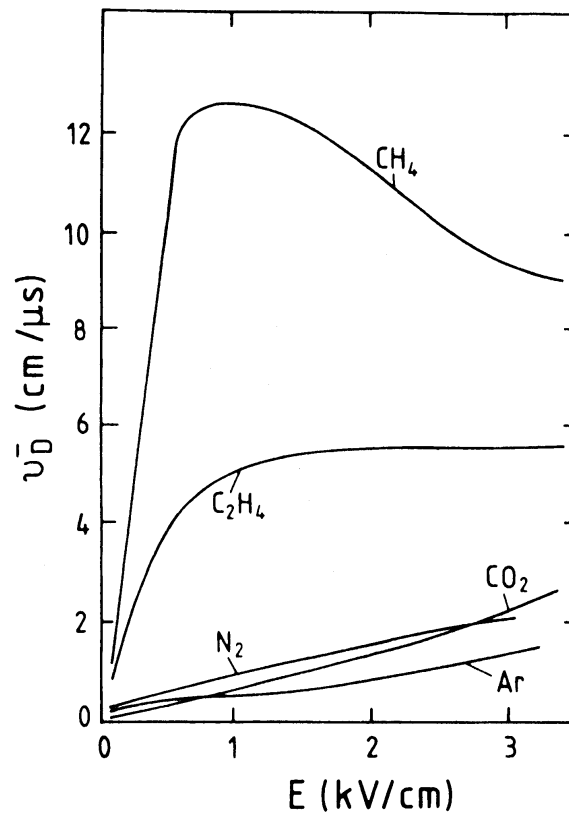
where the mobility μ is determined at standard pressure p_0 .

The drift velocity is often plotted vs. the reduced field E/p .

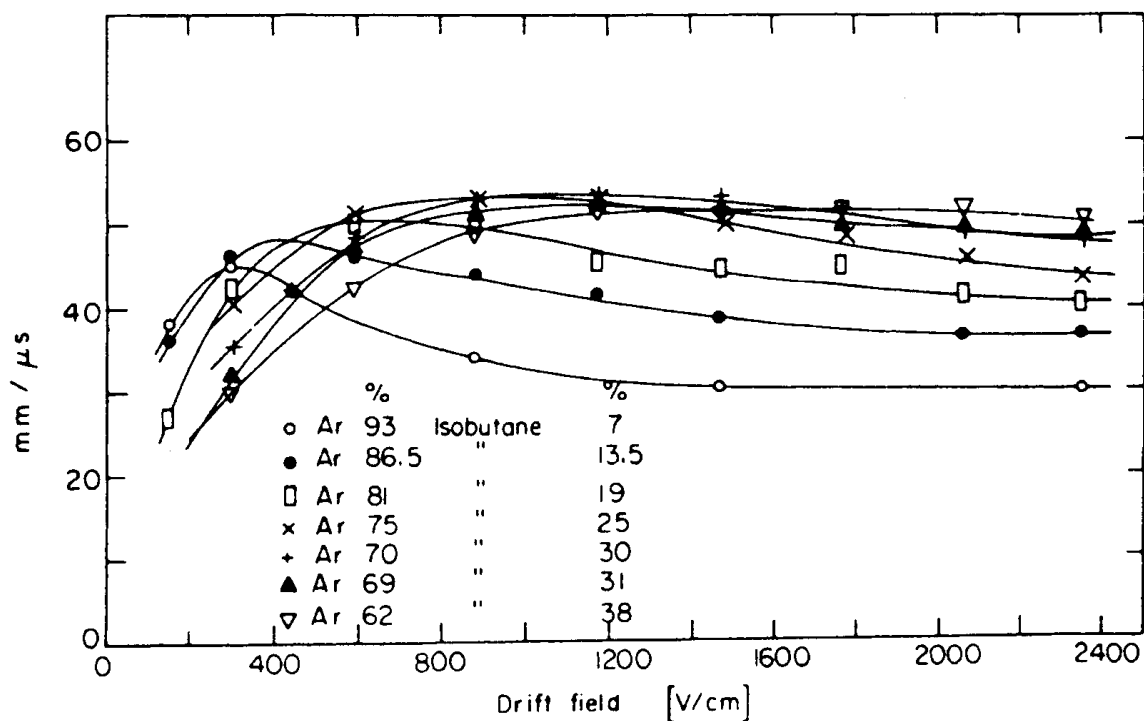
In reality the collision cross section is energy dependent, so this simple relationship does not hold over the full range of fields (i.e. electron energy).



At electron energies of ~ 0.1 eV the gas becomes nearly transparent, so acceleration is large, but then decreases at higher electron energies.

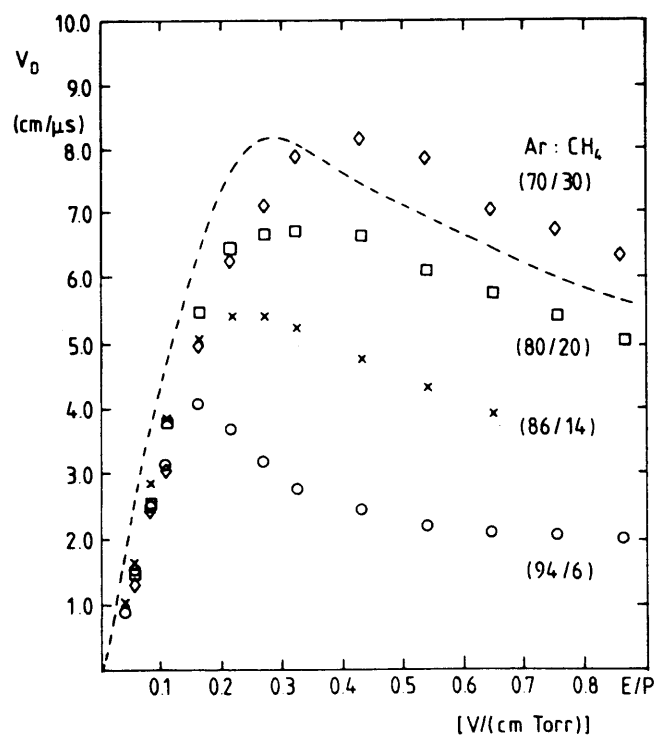


Electron velocity vs. drift field for various mixtures of Argon and Isobutane.



Electron velocity vs. E/p
for various mixtures of
Ar and CH₄.

The dashed
line is a calculation.



Electrons can be captured by molecules of electronegative gases such as O_2 , Cl_2^- , NH_3 and H_2O , leading to a loss in signal.

In gases such as N_2 , H_2 and CH_4 capture is negligible, but it is important to control gas purity to avoid deleterious trace contamination by electronegative impurities.

b) Drift velocity of ions

The drift velocity of ions is given by a similar expression as derived above

$$v^+ = \mu^+ E \frac{P_0}{p}$$

Since the ions are quite massive, the collision cross section remains constant.

For a gas mixture

$$\frac{1}{\mu} = \sum_k \frac{c_k}{\mu_k}$$

where μ_k and c_k are the mobility and concentration by volume of constituent k .

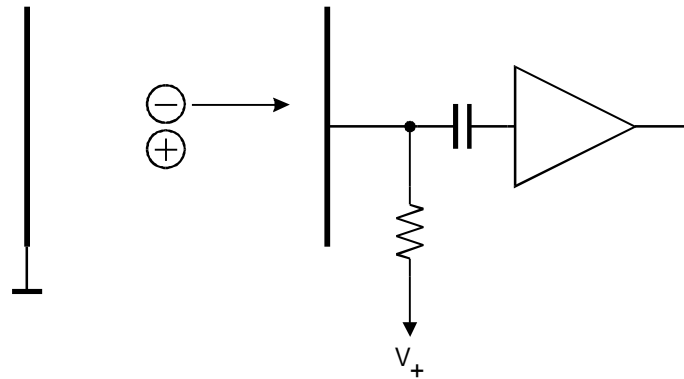
Measured mobilities of ions in various gases

Gas	Ion	Mobility [cm^2/Vs]
He	He^+	10.2
Ar	Ar^+	1.7
Ar	$(OCH_3)_2CH_2^+$	1.51
Iso- C_4H_{10}	$(OCH_3)_2CH_2^+$	0.55
$(OCH_3)_2CH_2$	$(OCH_3)_2CH_2^+$	0.26
Iso- C_4H_{10}	$IsoC_4H_{10}^+$	0.61
Ar	CH_4^+	1.87
CH_4	CH_4^+	2.26
Ar	CO_2^+	1.72
CO_2	CO_2^+	1.09

At 1 kV/cm ions are of order 1000 times slower than electrons.

1. Parallel Plate Ionization Chamber

Consider a simple parallel plate ionization chamber with an electrode spacing of 1 cm, operated at a voltage of 1 kV.



At a field of 10^3 V/cm the electron velocity is typically 10^6 cm/s, whereas the ion velocity is roughly 10^3 cm/s.

Electrons requires $1 \mu\text{s}$ to traverse the full detector volume; the ions take 1000 times longer, i.e. 1 ms.

Assume the integration time of the pulse processor is set to $1 \mu\text{s}$, to accommodate the maximum collection of the electrons. Within this time interval the ions will only move

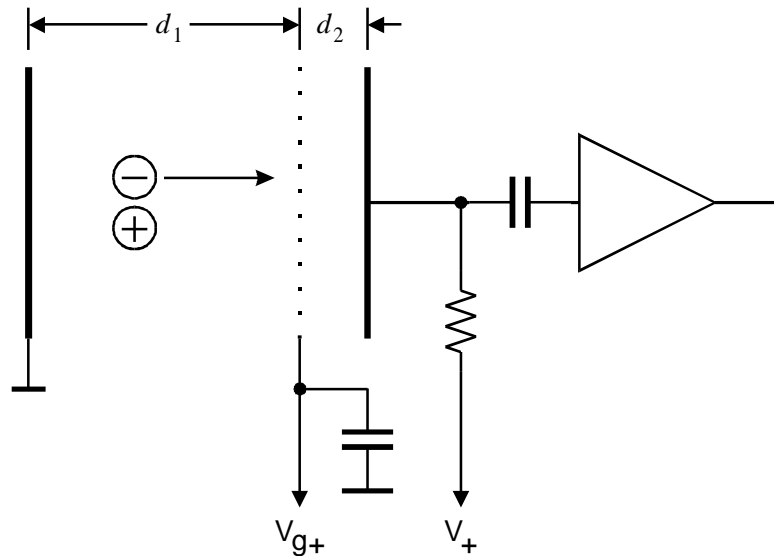
$$\Delta x = vt_{\text{int}} = 10^3 \cdot 10^{-6} = 10^{-3} \text{ cm}$$

so the induced charge

$$\Delta Q = Nq_e \frac{\Delta x}{d} = 10^{-3} Nq_e$$

Since the induced charge due to electrons can range from 0 to Nq_e , depending on the origin of the electron-ion pair, the obtainable energy resolution will be much worse than expected from the statistics of electron-ion formation.

The position dependence of the induced charge can be eliminated (practically) by introduction of a shielding grid (Frish grid).



Charges moving in the space d_1 between the grid and the left electrode induce current on these two electrodes, but not on the signal electrode.

When electrons move into the region d_2 between the grid and the signal electrode, they induce current on the signal electrode.

The two regions d_1 and d_2 constitute separate volumes for induced currents, i.e. the induced currents flow in two distinct loops.

Depending on the point of origin, the electrons drifting induce the charge

$$\Delta Q_1 = Nq_e \frac{\Delta x}{d_1}$$

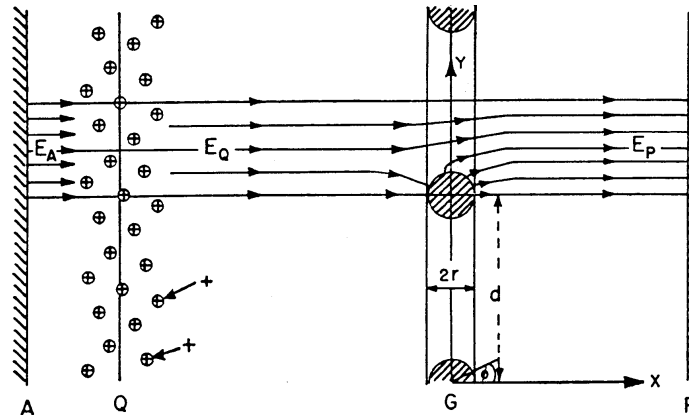
in the circuit defined by the left electrode and the grid. However, all electrons passing through the grid and traversing the region d_2 will induce

$$\Delta Q_2 = Nq_e \frac{d_2}{d_2} = Nq_e$$

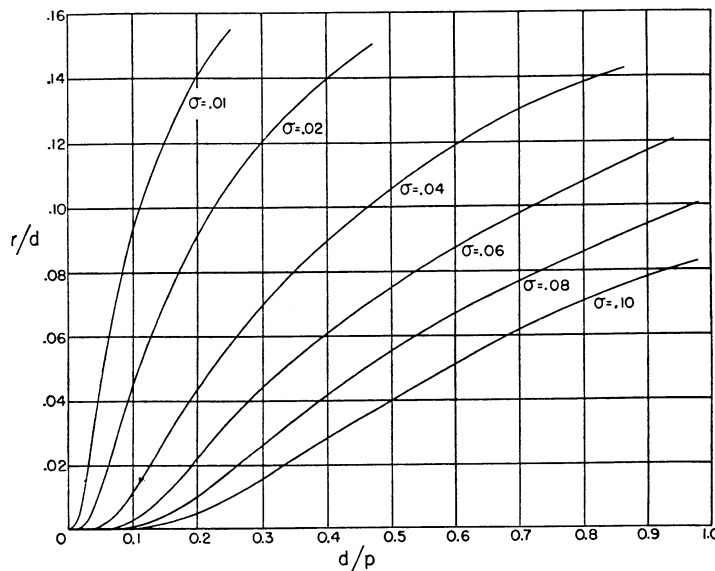
in the circuit defined by the grid and the signal electrode, so the full signal charge is induced for all charges originating in the region d_1 .

If the grid is made sufficiently dense to be an effective electric shield, will the electrons still pass through it?

By appropriate choice of geometry and grid potential the efficiency of electron transmission can be $\sim 100\%$.



Inefficiency of shielding σ vs. wire radius/pitch r/d and ratio of pitch to grid position d/p (p is d_2 on the previous page).



Rather dense grids are needed for good shielding.

By increasing the potential between the grid G and the collection electrode P such that the field E_P is greater than E_Q , the grid can be made increasingly transmissive for electrons. Depending on the grid geometry, ratios $E_P/E_Q \approx 2 - 3$ will provide $\sim 100\%$ transmission

(Bunemann et al., Canadian J. of Res. **27A** (1949) 191)

2. Proportional Chambers

At high electric fields electrons can acquire sufficient energy between collisions to ionize gas molecules. As discussed for photodiodes, this mechanism can be exploited to increase the signal from the detector.

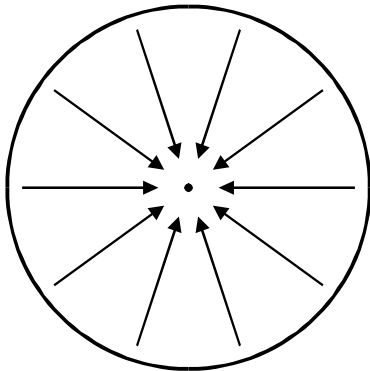
The probability of ionization is determined by the “first Townsend coefficient” α . The increase in the number of electrons traversing an increment dx is

$$dN = N \alpha dx$$

In a uniform electric field the signal gain over a distance L is

$$G = \frac{N}{N_0} = e^{\alpha L}$$

High fields are typically obtained by utilizing the radial dependence of the electric field near a thin wire.



In a coaxial geometry with an applied voltage V_b the field

$$E(r) = \frac{V_b}{r \ln \frac{r_2}{r_1}}$$

where r_1 is the inner and r_2 the outer radius.

Typical wire diameters for the inner conductor are 25 – 50 μm .

If the gas gain is to be the same for all signals, the volume of the multiplication region must be negligible compared to the total detection volume.

Assume that the field required for the onset of appreciable ionization is 50 kV/cm (“critical field”). The radius at which appreciable ionization sets in is

$$r_c = \frac{V_b}{E_c \ln \frac{r_2}{r_1}}$$

If the wire diameter is 25 μm and the outer radius is 25 mm, and 1 kV is applied to the chamber, the critical radius is about 30 μm .

⇒ The avalanche region is about 10^{-6} of the chamber volume.

The total avalanche gain is determined from

$$\int \frac{dN}{N} = \int_{r_c}^{r_1} \alpha(r) dr$$

The integral is taken from radius at which appreciable avalanching sets in to the radius of the inner electrode.

Since the ionization coefficient is primarily a function of field, the dependence of field vs. radius must be introduced. This yields the expression for the gas gain

$$\ln G = \int_{r_c}^{r_1} \alpha(r) dr = \int_{E(r_c)}^{E(r_1)} \alpha(E) \frac{dr}{dE} dE$$

The ionization coefficient α is a function of field. Furthermore, the probability of ionization depends on the mean free path, i.e. the gas pressure p . It is found experimentally that for a given E/p , α is proportional to p .

$$\alpha = f(E/p) \cdot p$$

For noble gases in the range of fields appropriate for proportional chambers, one can use the Diethorn approximation

$$\alpha(E) \approx \beta E$$

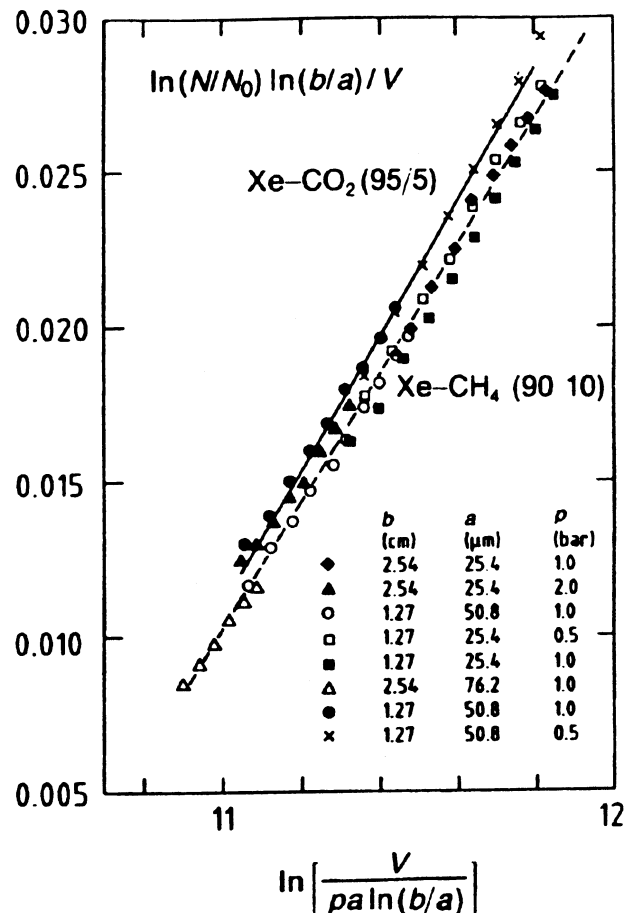
where β depends on the ionization energy ε_i

$$\beta = \frac{\ln 2}{\varepsilon_i}$$

Combining the above expressions yields the gas gain

$$\ln G = \frac{\ln 2}{\varepsilon_i} \frac{V_b}{\ln(r_2/r_1)} \ln \frac{V_b}{\ln(r_2/r_1) \cdot r_1 E(r_c, p) (p/p_0)}$$

A plot of $\ln(N/N_0) \ln(r_2/r_1) / V$ vs. $\ln[V/(pr_1 \ln(r_2/r_1))]$ shows that data points for all geometries and voltages lie on curves specific to the gas.



The parameters ε_i and $E(r_c)$ are characteristic of the specific gas.

Gas mixture	$E(r_c)$ [kV/cm]	ε_i [Volts]
90% Ar + 10% CH ₄	48 ± 3	23.6 ± 5.4
95% Ar + 5% CH ₄	45 ± 4	21.8 ± 4.4
92.1% Ar + 7.9% CH ₄	47.5	30.2
23.5% Ar + 76.5% CH ₄	196	36.2
9.7% Ar + 90.3% CH ₄	21.8	28.3
0.2% Ar + 99.8% CH ₄	171	38.3
CH ₄ (Hendricks)	69 ± 5	36.5 ± 5.0
CH ₄ (Diethorn)	144	40.3
C ₃ H ₈	100 ± 4	29.5 ± 2.0
75% Ar + 15% Xe + 10% CO ₂	51 ± 4	20.2 ± 0.3
90% Xe + 10% CH ₄	36.2	33.9
95% Xe + 5% CO ₂	36.6	31.4

Induced Signal

The avalanche forms both electrons and ions. The electrons drift towards the inner wire and the ions towards the outer electrode.

The electrons only drift a short distance (10s of μm), but the $1/r$ dependence of the weighting field increases their contribution.

Assume N electrons and ions formed at radius r . The weighting potential for the induced charge is

$$\Phi_Q = \int F(r)dr = \frac{1}{\ln(r_2 / r_1)} \int \frac{1}{r} dr = \frac{\ln r}{\ln(r_2 / r_1)}$$

so the induced charge due to electrons and ions

$$Q_{s,el} = -Nq_e (\Phi_Q(r_1) - \Phi_Q(r)) = Nq_e \frac{\ln(r / r_1)}{\ln(r_2 / r_1)}$$

$$Q_{s,ions} = Nq_e (\Phi_Q(r_2) - \Phi_Q(r)) = Nq_e \frac{\ln(r_2 / r)}{\ln(r_2 / r_1)}$$

The ratio of induced charges

$$\frac{Q_{s,el}}{Q_{s,ions}} = \frac{\ln(r/r_1)}{\ln(r_2/r)}$$

Since the avalanche builds up within 10s of microns of the inner conductor $r/r_1 < 2$, whereas r_2/r is of order 1000

$$\frac{Q_{s,el}}{Q_{s,ions}} < \frac{\ln(2)}{\ln(1000)} = 0.1$$

The total charge signal is dominated by the motion of the ions.

However, since the induced current

$$i_s = Nq_e v(r) F(r) = Nq_e \mu(E) E(r) F(r)$$

$$i_s = Nq_e \mu(E) \frac{V}{(\ln(r_2/r_1))^2} \frac{1}{r^2} \propto \frac{\mu(E)}{r^2}$$

the electron current is orders of magnitude greater than the ion current, due to the greater mobility of the electrons and the fact that they are moving at very small radii.

Hence, the signal current has a fast and large component due to the electrons superimposed on the ion current, which is much smaller, but orders of magnitude longer. Since the electron component may be less than 1 ns in duration, very fast electronics and low-inductance chamber design are needed to utilize (or even see) it.

The long drift time of the ions limits the rate capability of proportional chambers.

At high rates the accumulated space charge from the ions distorts the electric field and reduces the gain.

The use of small gas volumes that restrict the maximum ion drift distance increases the rate capability.

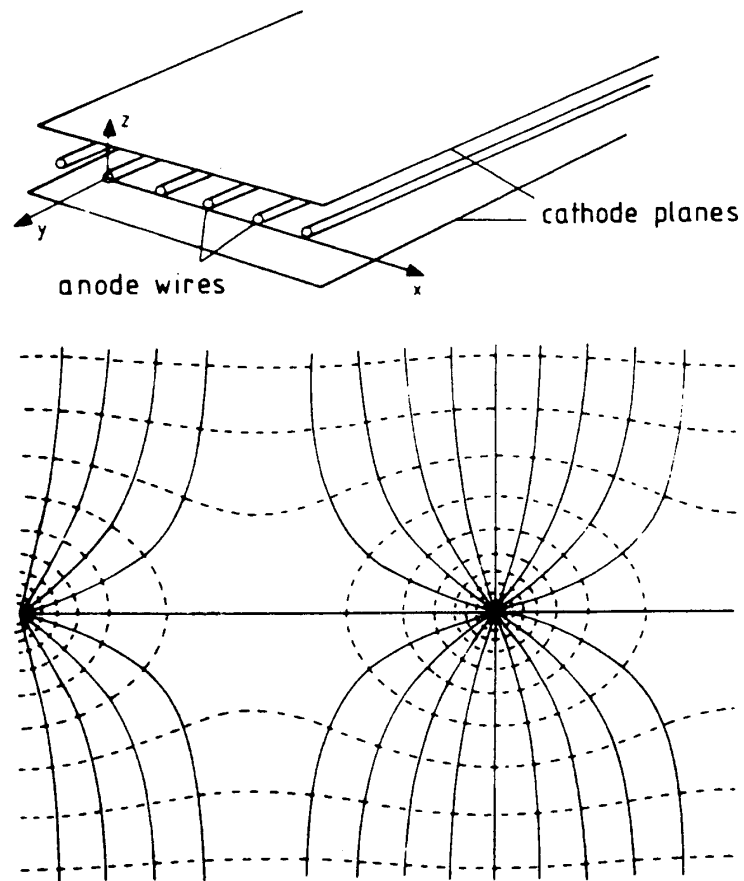
Example: "straw" tubes with an outer diameter of several mm allow rates of $>10^7 \text{ s}^{-1}$.

Position Sensitive Detectors

1. Multi-Wire Proportional Chamber (MWPC)

An array of many thin wires forms a multi-channel proportional chamber.

Electrode configuration and field distribution



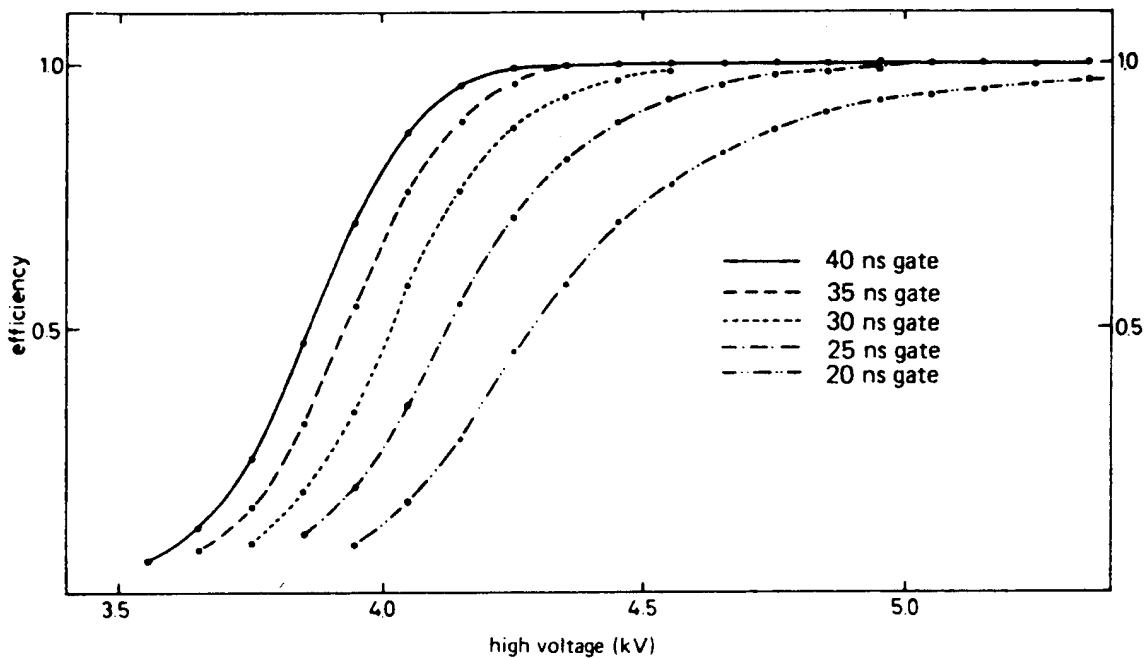
The field near the wires depends primarily on the wire radius.

Many cathode geometries possible.

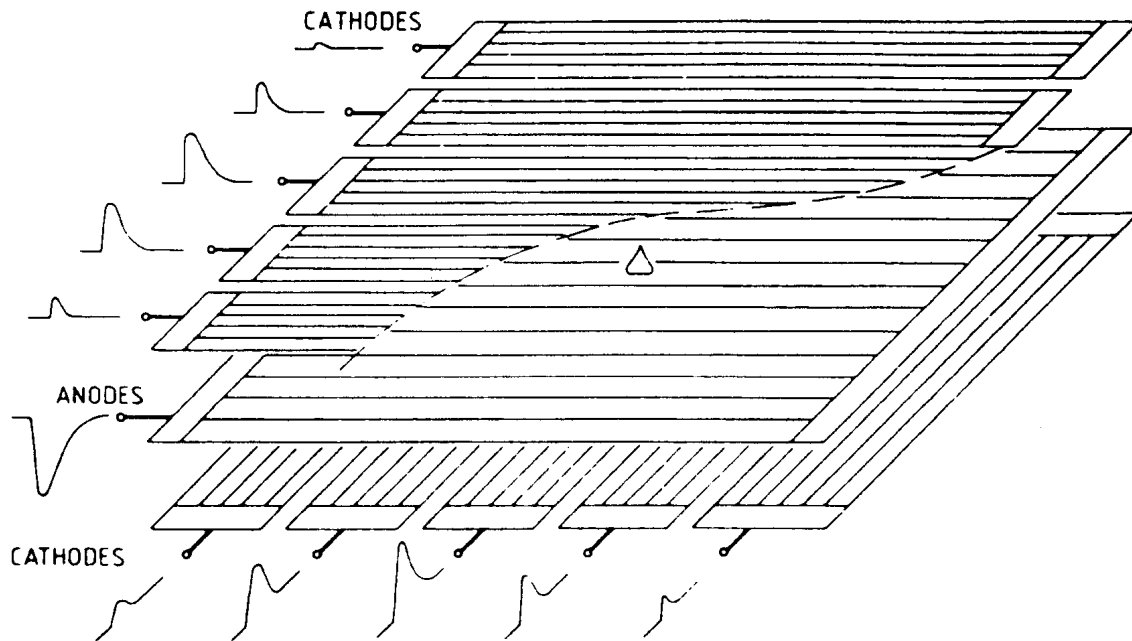
MWPCs are often used with simple threshold discrimination, where the presence of a “hit” (signal above threshold) indicates the location of a particle.

The integration time of the pulse processing preceding the threshold discriminator determines the fraction of the signal charge that is registered.

Dependence of efficiency vs. integration time (“gate”) and applied voltage.



The cathode planes can be segmented to provide additional position sensing.



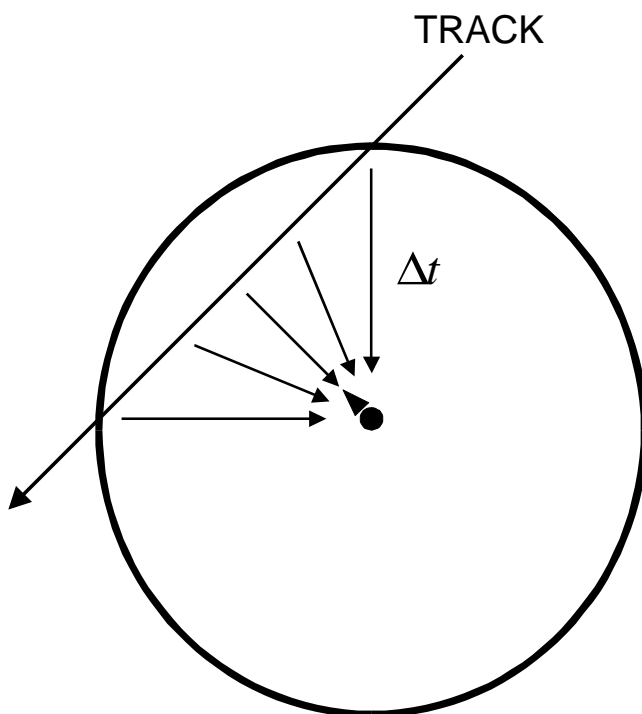
(from Charpak)

The lower cathode plane provides position sensing along the wires. Evaluation of the pulse height distribution allows interpolation to better than the pitch of the cathode pads.

2. Drift Chambers

In systems where an external time reference is available, the time required for primary charges to reach the avalanche region can be used for position sensing.

Example: “straw” chamber



Electrons formed along the track drift towards the central wire. The first electron to reach the high-field region initiates the avalanche, which is used to derive the timing pulse.

Since the initiation of the avalanche is delayed by the transit time of the charge from the track to the wire, the time of the avalanche can be used to determine the position.

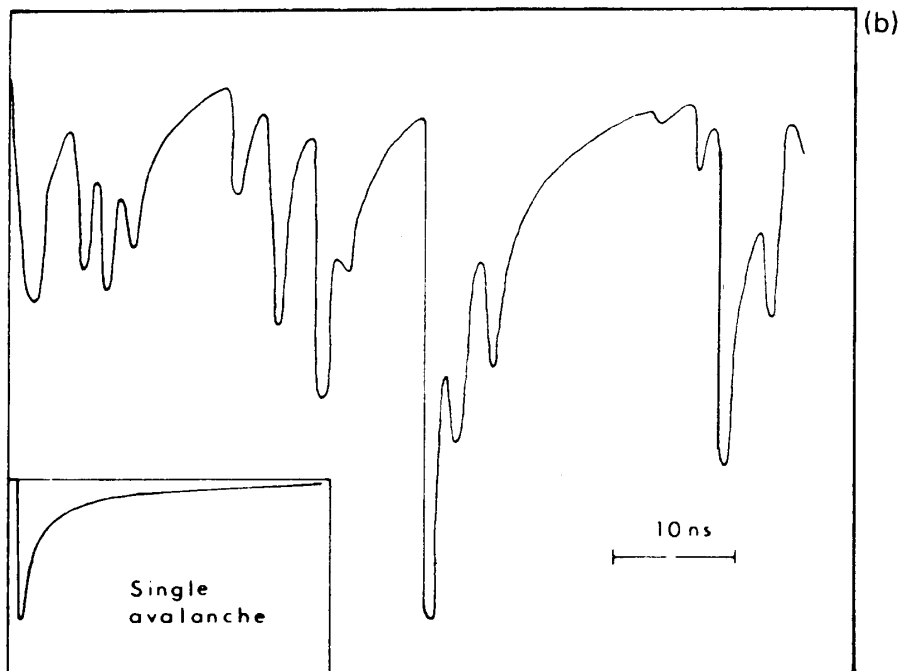
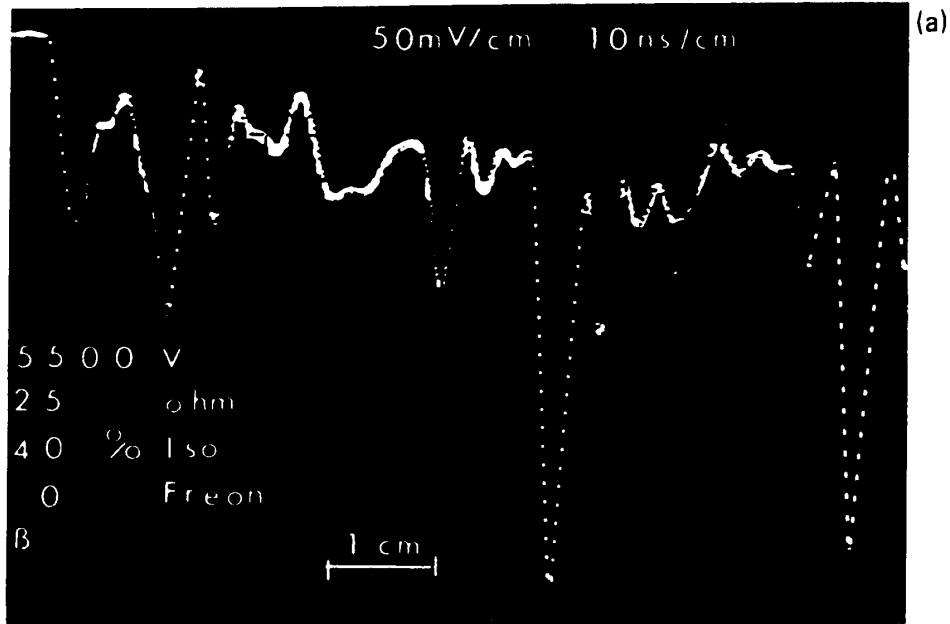
Achievable position resolutions are $\sim 100 \mu\text{m}$.

Minimum ionizing particles deposit energy in clusters along the track, so the point of minimum distance does not necessarily coincide with a cluster.

⇒ Pulses have significant time structure (trigger on first pulse)

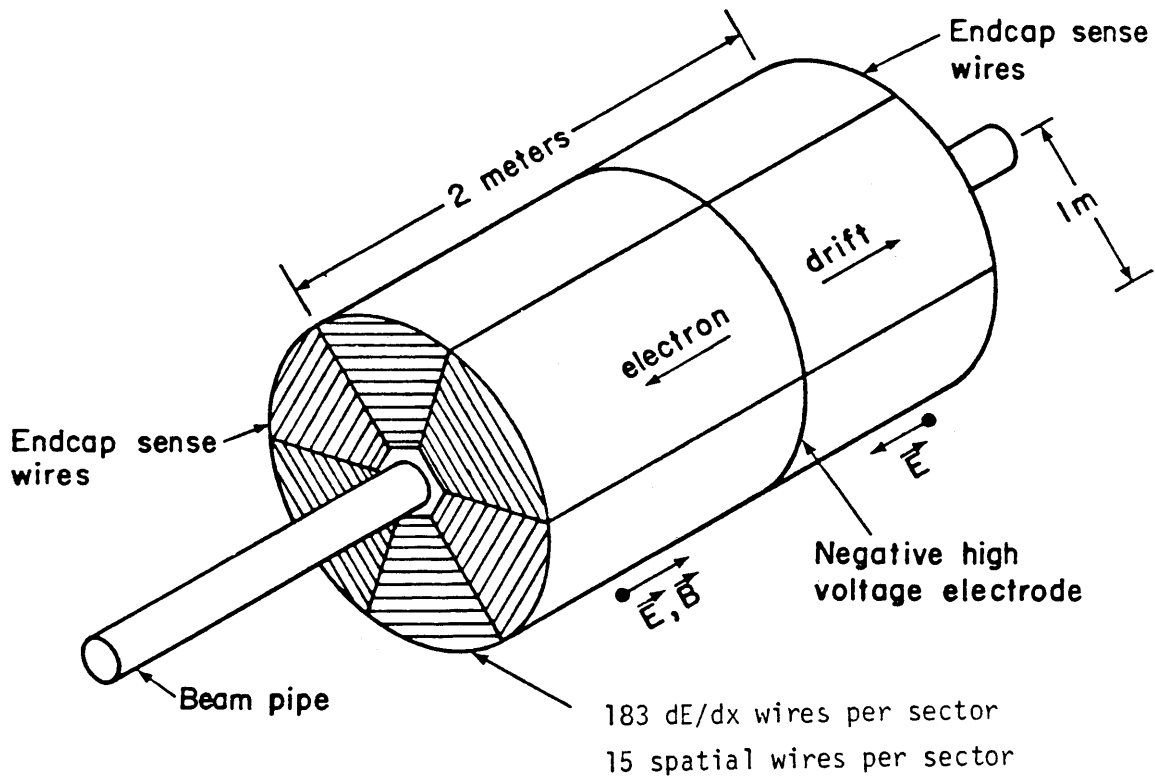
Top: measured

Bottom: simulated



3. Time Projection Chamber (TPC)

The TPC utilizes the principle of a drift chamber on a large scale to provide 3D imaging.



(M.D. Shapiro, thesis, 1984)

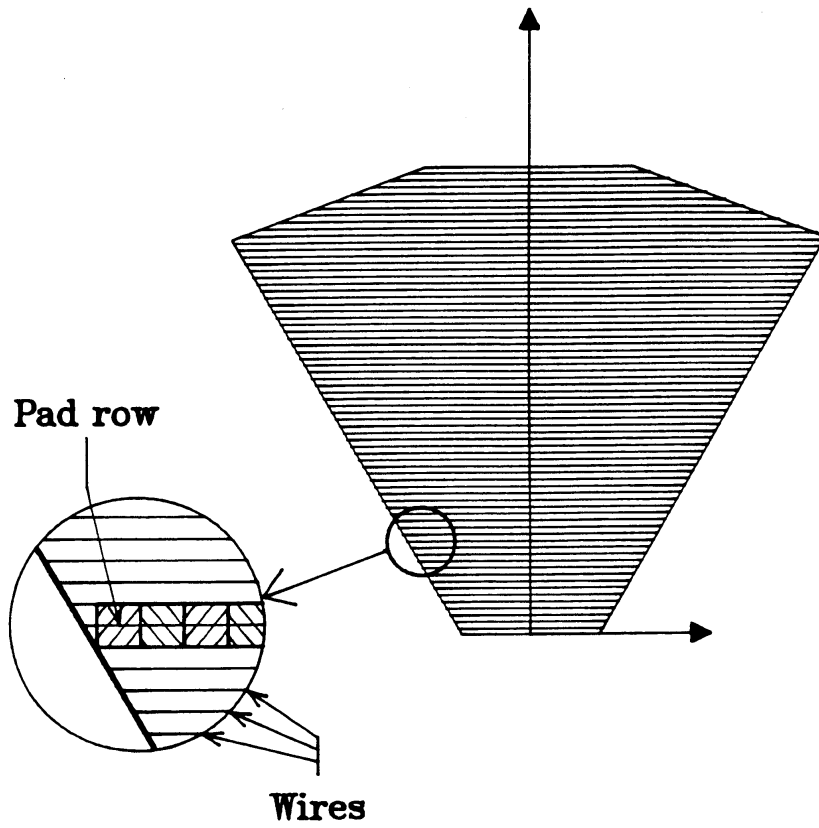
Electrons drift through a large volume to the endcaps, where they avalanche at a grid of wires.

The drift time provides the longitudinal coordinate,

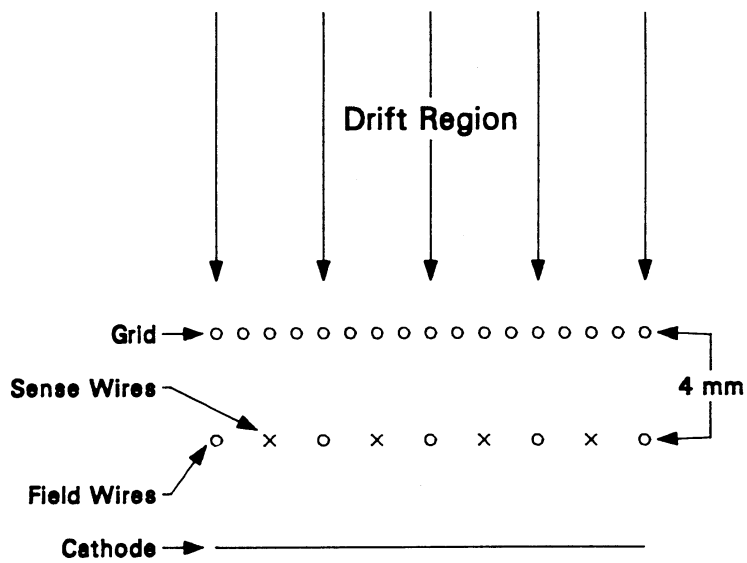
The wires the radial coordinate.

Pads arranged along the wires provide the ϕ coordinate.

Detail of endcap sector

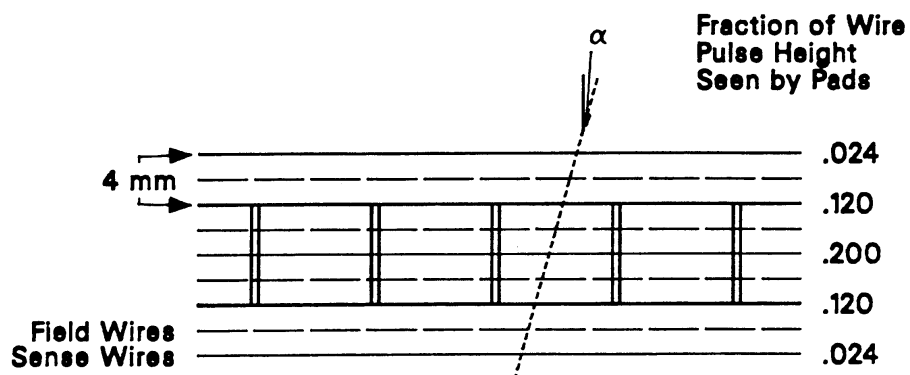


A combination of grids provides field shaping
avalanching
signal sensing

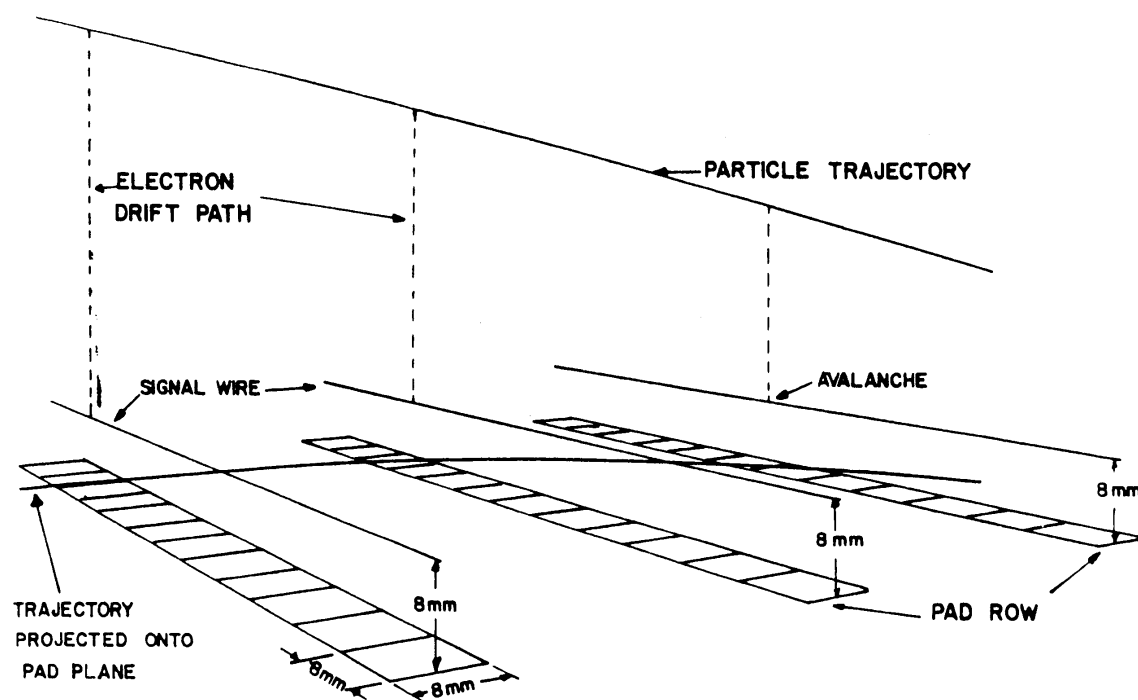


The cathode plane is segmented with rows of pads along the avalanche wires to provide position resolution along the wires.

Analog interpolation improves the resolution in both coordinates.



The projection of a particle track on the endcap together with the longitudinal drift time provides true 3D space points.



At first glance this device would seem to be unworkable, as transverse diffusion will spread the charge radially with a Gaussian distribution

$$n(r) = \left(\frac{1}{\sqrt{4\pi Dt}} \right)^3 \exp\left(-\frac{r^2}{4Dt} \right)$$

The standard deviation after drifting a distance x

$$\sigma_r = \sqrt{Dt} = \sqrt{\frac{2\varepsilon_k x}{q_e E}}$$

where ε_k is a characteristic energy of the electron ($> (3/2)k_B T$)

The long drift times (10s of μs) would ruin the r and $r\phi$ resolution.

The key insight (D. Nygren) was that a magnetic field parallel to the electric drift field reduces transverse diffusion.

The transverse diffusion coefficient is reduced by a factor

$$\frac{1}{1 + \omega^2 \tau^2}$$

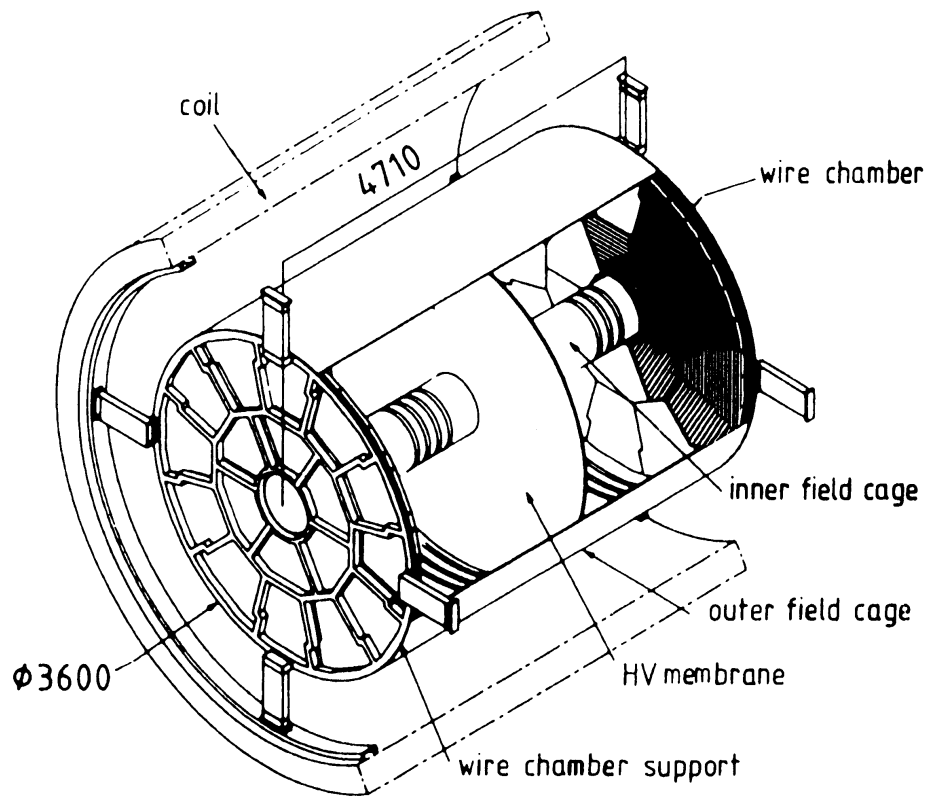
where $\omega = \frac{q_e B}{m}$ is the cyclotron frequency of the electrons and τ is

the mean time between collisions.

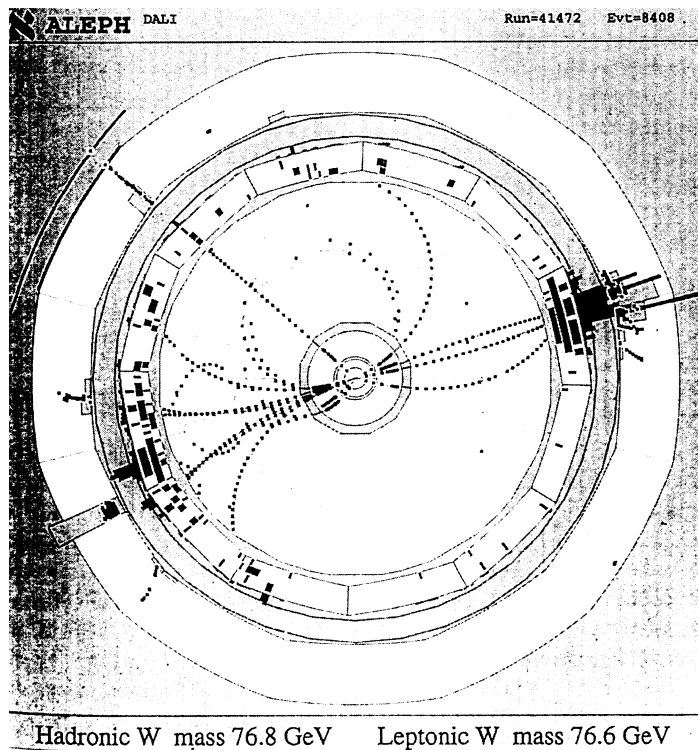
The centroid of a Gaussian distribution can be determined to a fraction of the standard deviation, depending on the number of charges in the cluster (segment of the track “captured” by a readout cell).

For a primary signal cluster with > 150 el the spatial resolution after 1 m drift at $B \approx 1$ T can be $< 200 \mu\text{m}$.

The largest TPC built to date is in the Aleph detector at CERN.



Typical event display

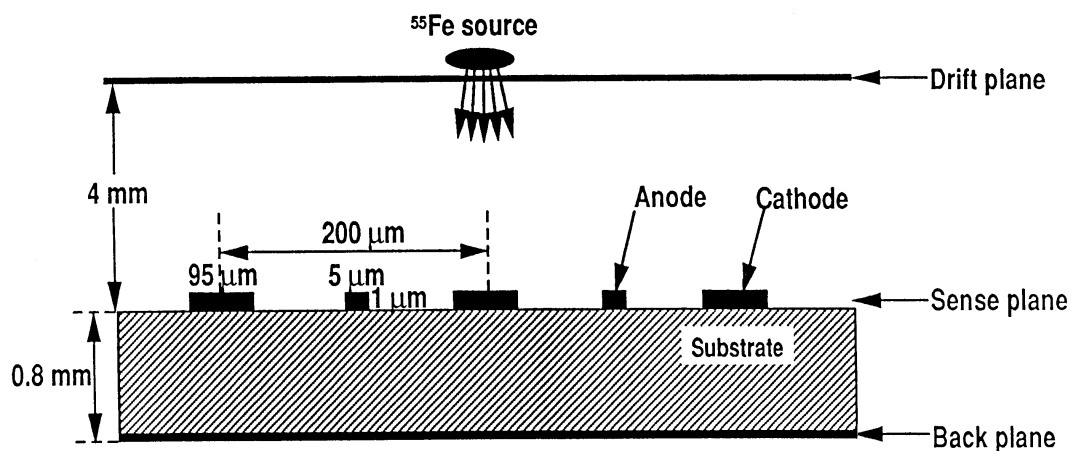


Rate limitations due to ion charge buildup can be mitigated by reducing the cell size. One of the advantages of Si is that characteristic dimensions are microns rather than mm.

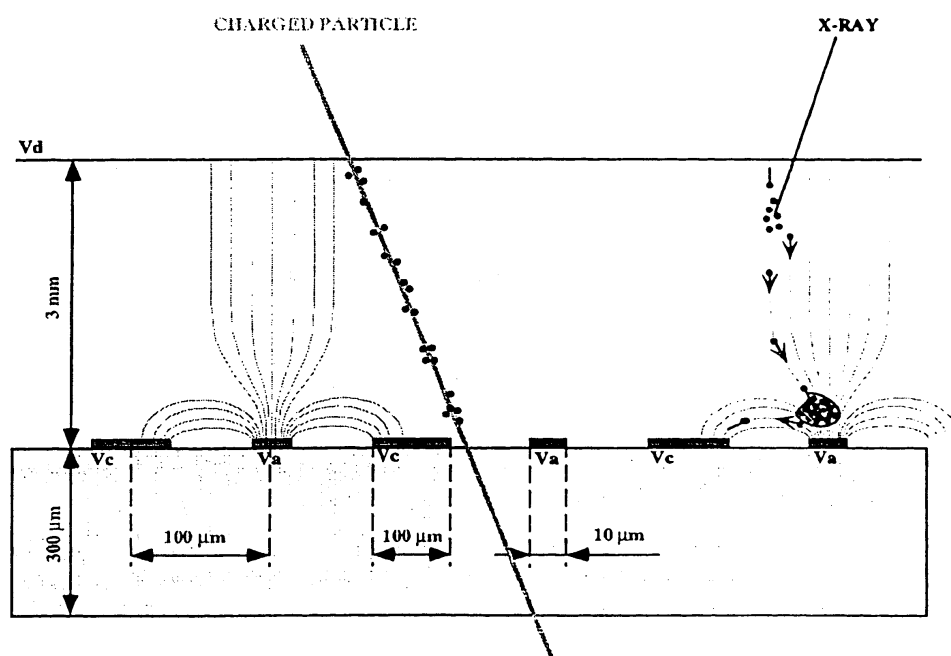
Recent developments in proportional chambers utilize technology from semiconductor fabrication to make micron-scale structures.

4.1. Micro-Strip Gas Chamber (MSGC)

MSGCs utilize strip anodes and cathodes on an insulating substrate.

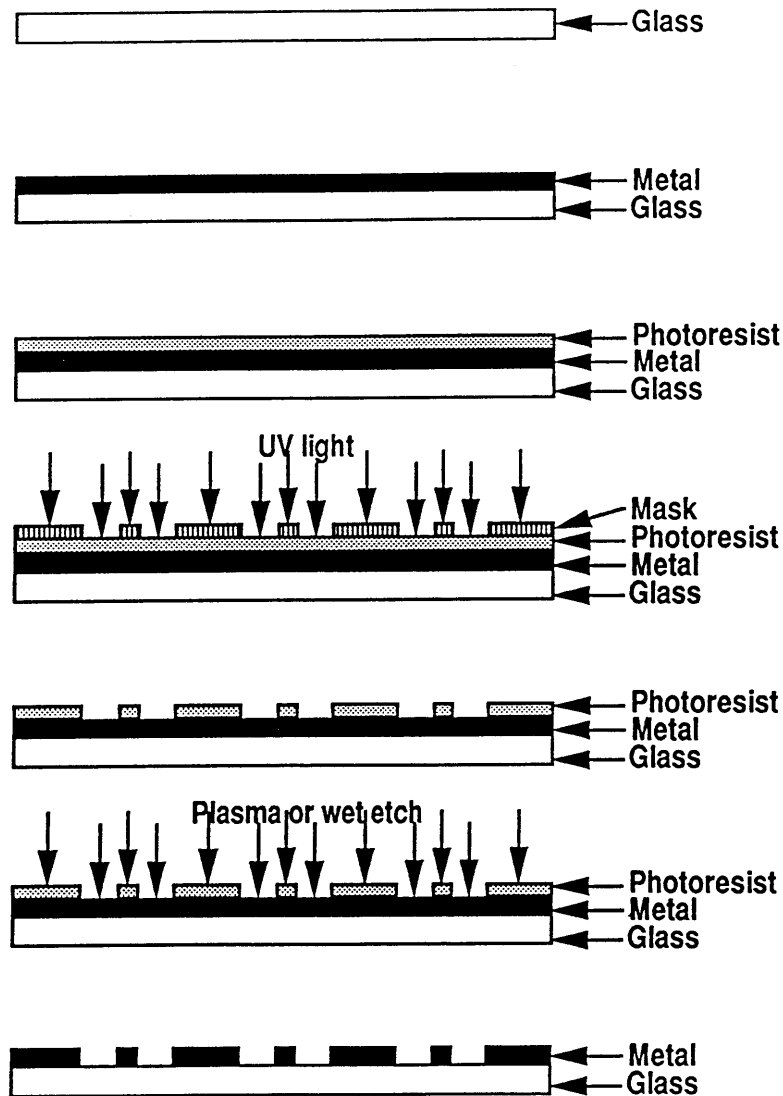


Electrons avalanche at the high field formed at the anode strips.



(from Hoch)

The electrodes are fabricated on a glass substrate using standard microfabrication techniques (photolithography + etching).

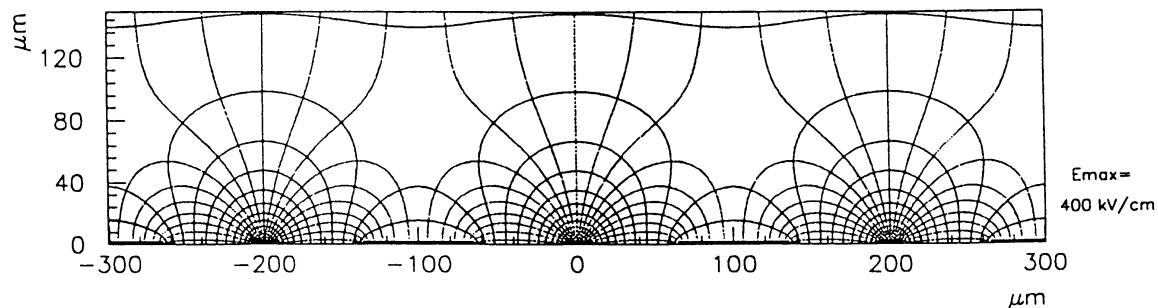


The properties of the substrate are critical. If it is perfectly insulating, charge builds up on the surface and changes the field.

Too large a surface conductivity will lead to excessive leakage current.

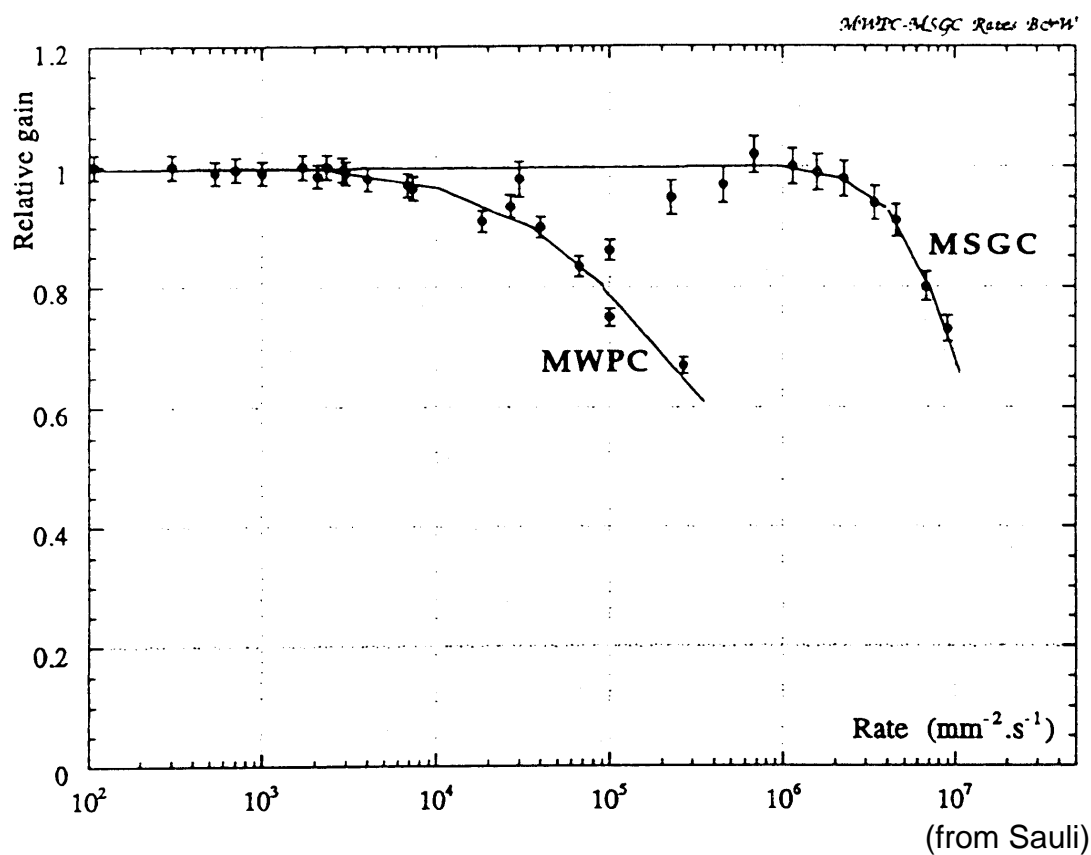
Since the distance between the anode and cathode is much smaller than in conventional wire chambers, the ions are collected more quickly.

Electric field distribution



(from Bellazzini)

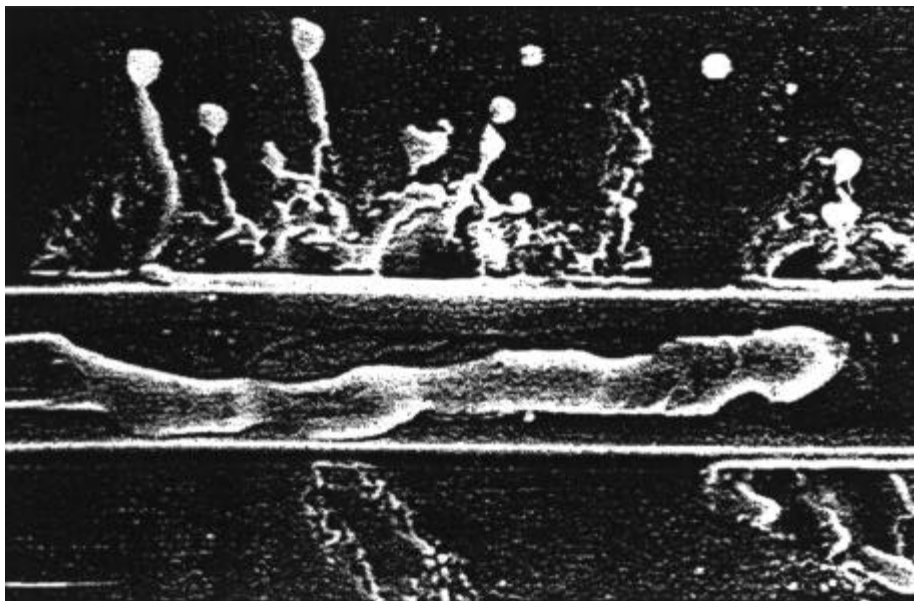
Because of the faster collection of the ions, the rate capability of an MSGC is superior to that of a multi-wire proportional chamber.



(from Sauli)

Proportional chambers are subject to two critical failure mechanisms:

1. Damage to a strip after sparking



This is an aluminum strip. Metals with higher melting points (e.g. tungsten) improve the resistance to damage from local discharge.

Sharp corners also form local high fields, so the electrodes must be rounded at the ends and corners. Important not to run at higher gain than necessary.

2. Aging

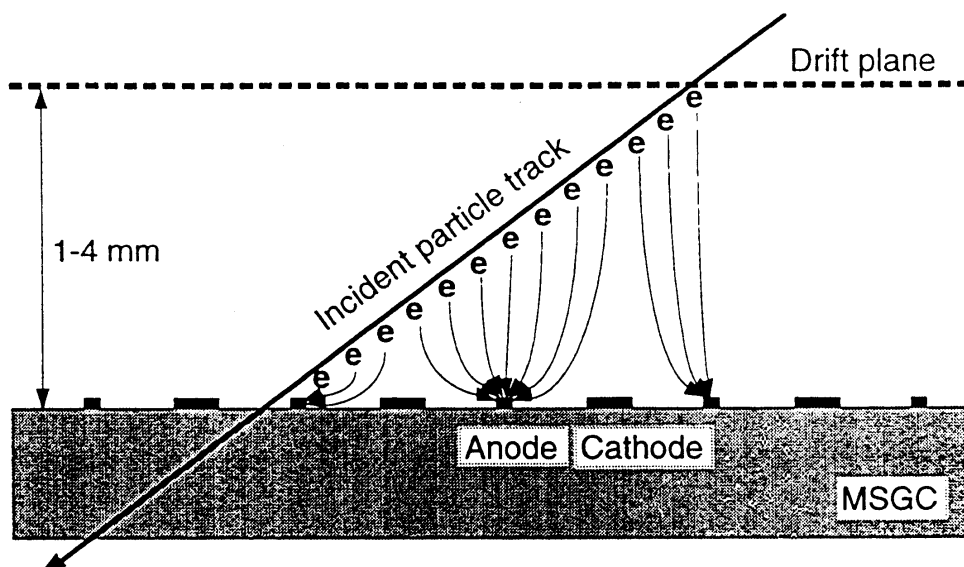
At high fields the hydrocarbons in many gases polymerize on the wires of MWPCs and strips of MSGCs, forming “whiskers” or “droplets” on the electrode. These deposits alter the field distribution and reduce detection efficiency with time.

Judicious choice of gas mixtures and operating conditions (especially low gas gain) can greatly alleviate this problem.

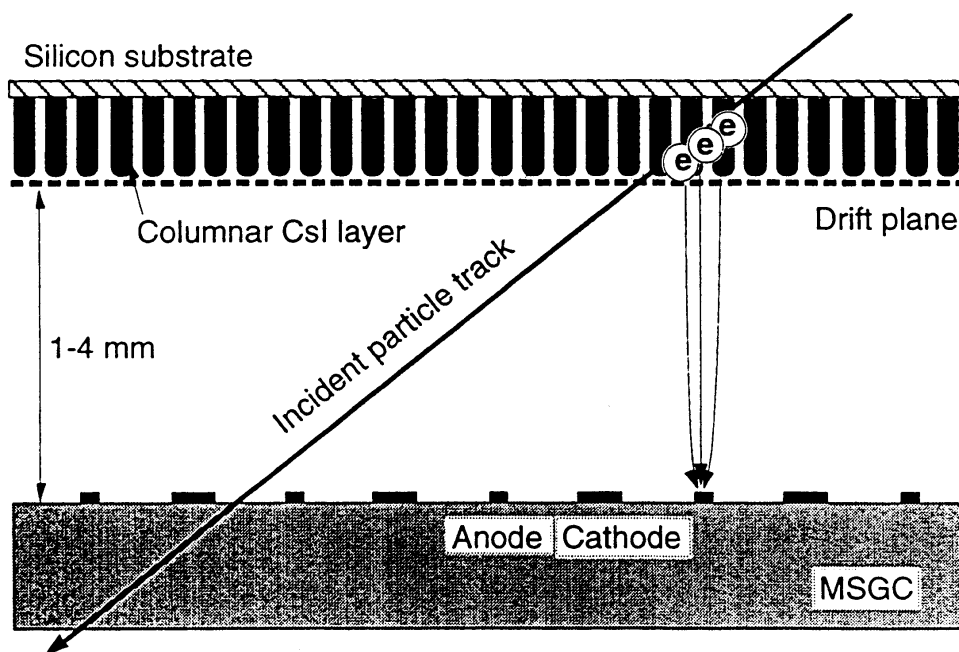
For a review see J. Kadyk, NIM A300(1991)436

Since the energy loss dE/dx in gases is smaller than in solids (lower density), the active absorption region must still be of order mm thick to obtain sufficient signal.

Tracks traversing the detector at an angle distribute charge on several strips.

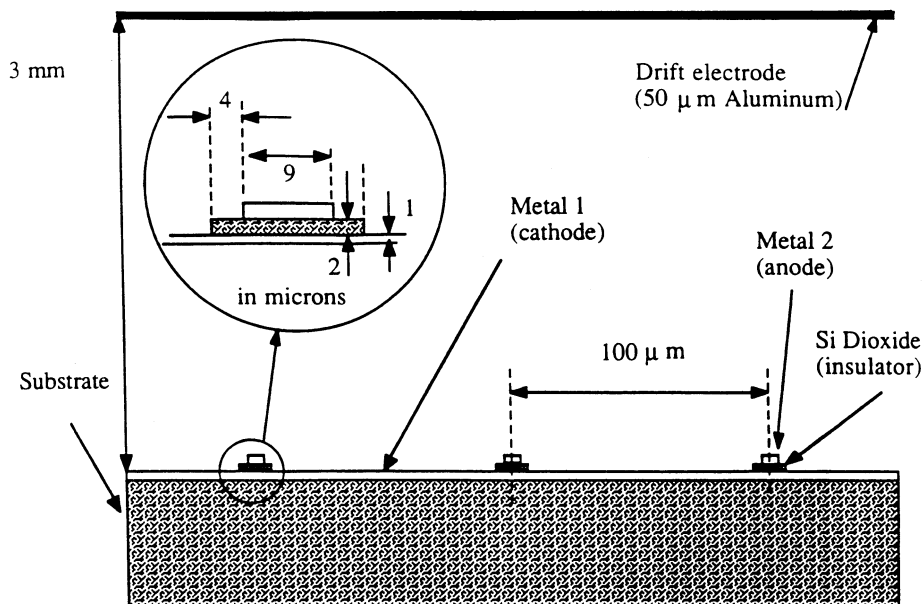


One proposed solution is to introduce an intermediate solid layer with higher dE/dx , in this example CsI grown as columnar microcrystals normal to the surface (Perez-Mendez).



4.2. Micro-Gap Chamber (MGC)

The micro-gap chamber reduces the path for ion collection even more.

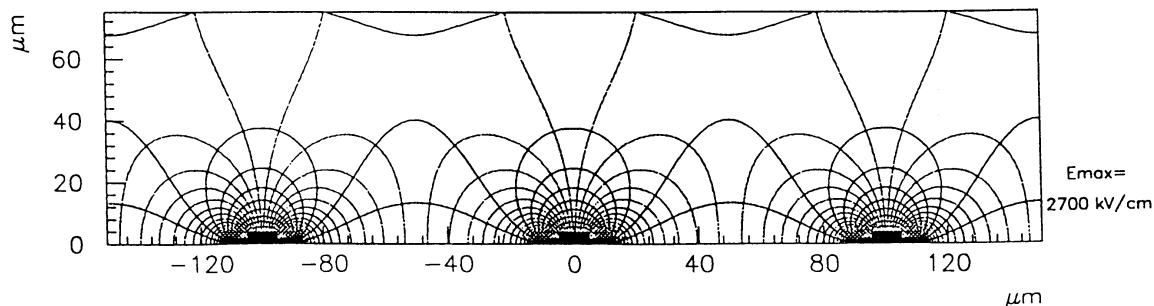


(from Bellazzini)

The cathode is a contiguous metal plane. The anodes are strips placed at a small distance (~ 2 microns) above the cathode plane, using thin strips of silicon-dioxide.

This geometry eliminates the problem of surface charging. The rate capability improves because the ions are collected within 10s of microns. These improvements come at the expense of added fabrication complexity.

Field distribution

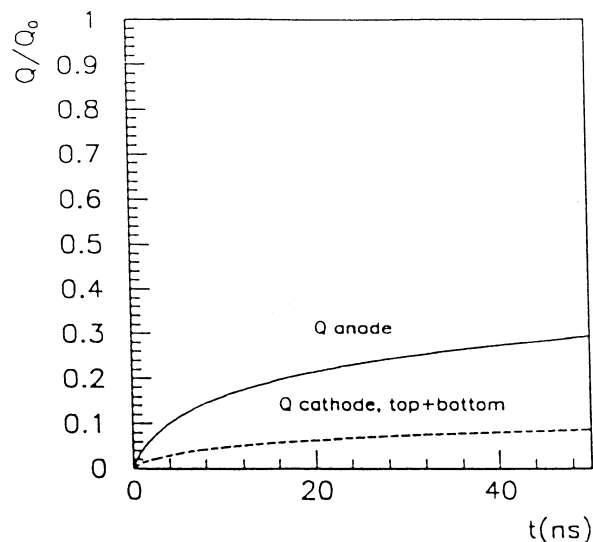


(from Bellazzini)

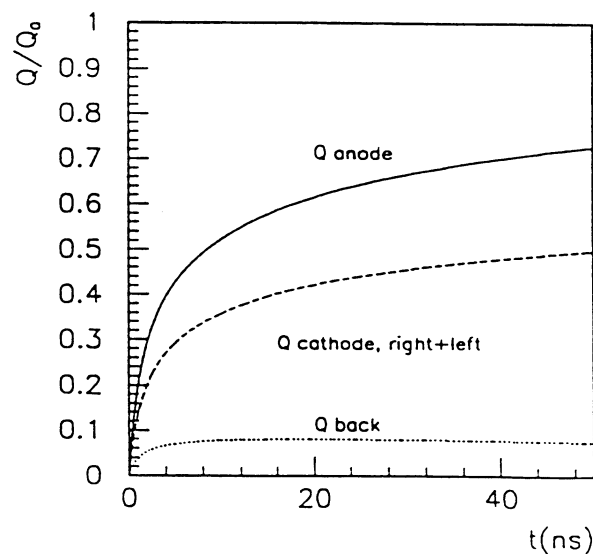
Induced signal due to electrons and holes vs. time
(from Bellazzini)

a) Multi-Wire Proportional Chamber

(symmetrical cathode planes above and below anode grid)

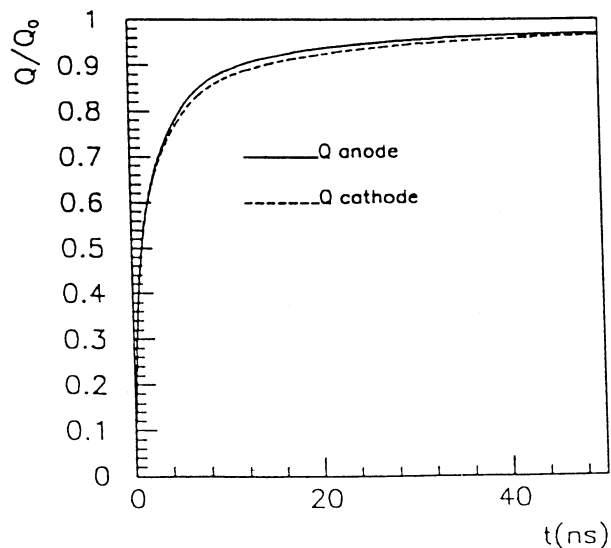


b) Micro-Strip Gas Chamber



c) Micro-Gap Chamber

The MGC has a relatively high capacitance. Since the primary signal is rather low, even with gas gain the signal-to-capacitance ratio is about the same as in Si strip detectors.

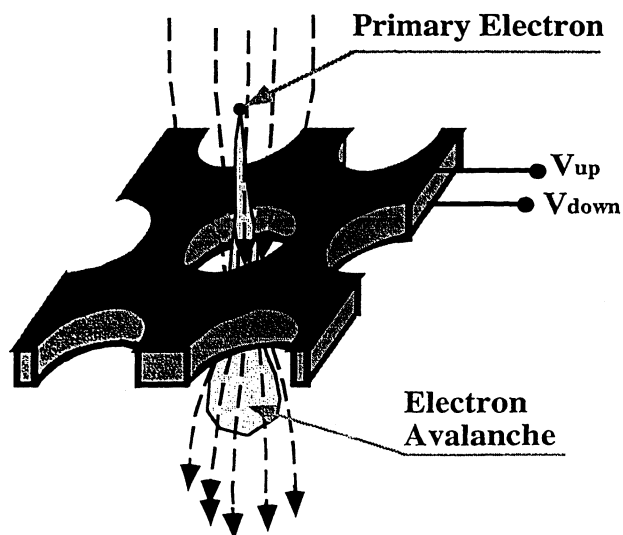


4.3. The Gas Electron Multiplier (GEM)

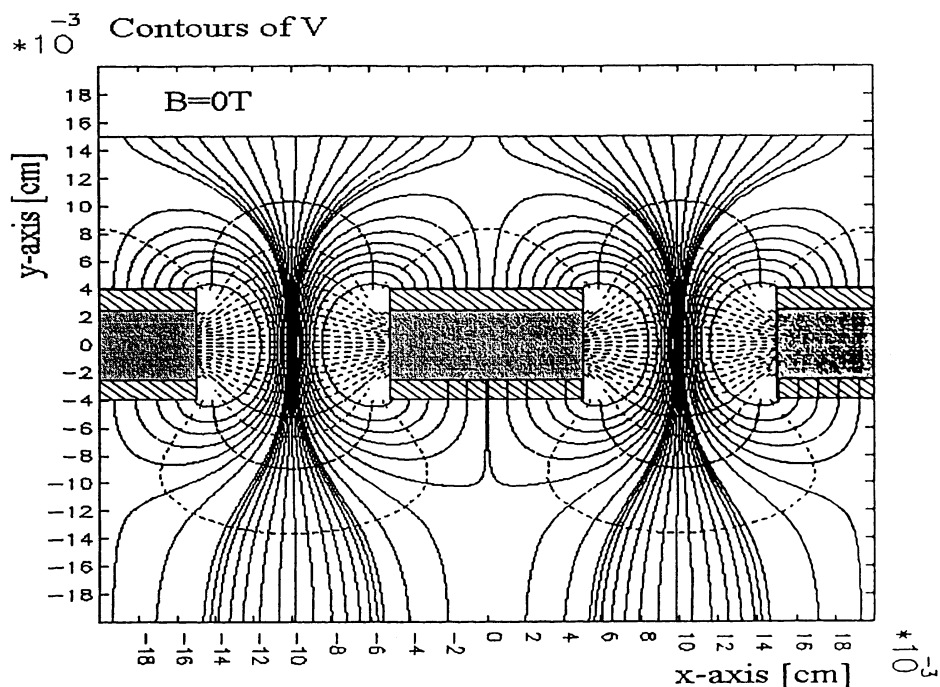
The gas electron multiplier a gain stage that can be combined with a variety of readout electrode structures.

The GEM consists of two electrodes formed by metal layers on both sides of a thin insulator (typically Kapton).

Perforations in this sandwich form local high field regions in which electrons avalanche in a gas.

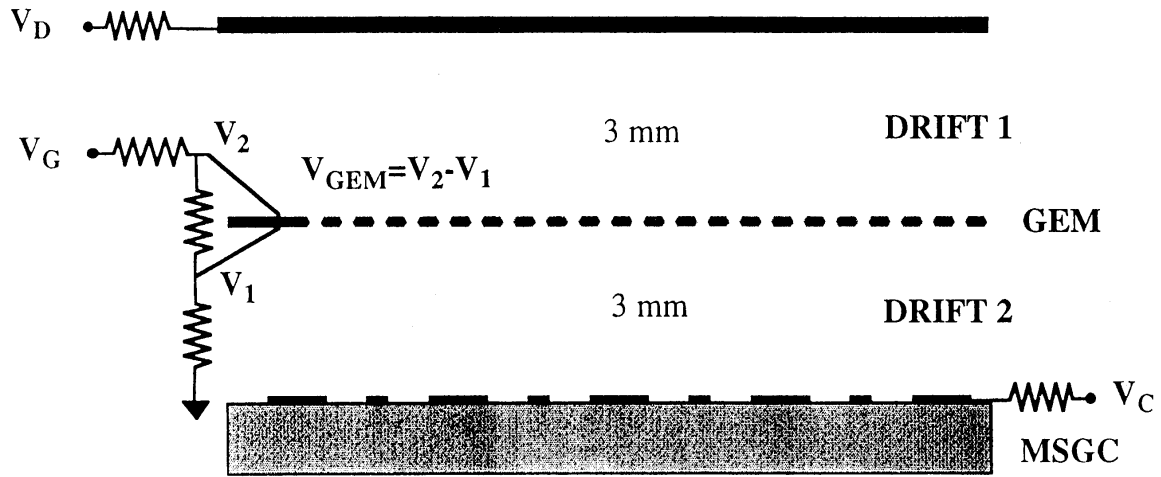


Field distribution in the aperture



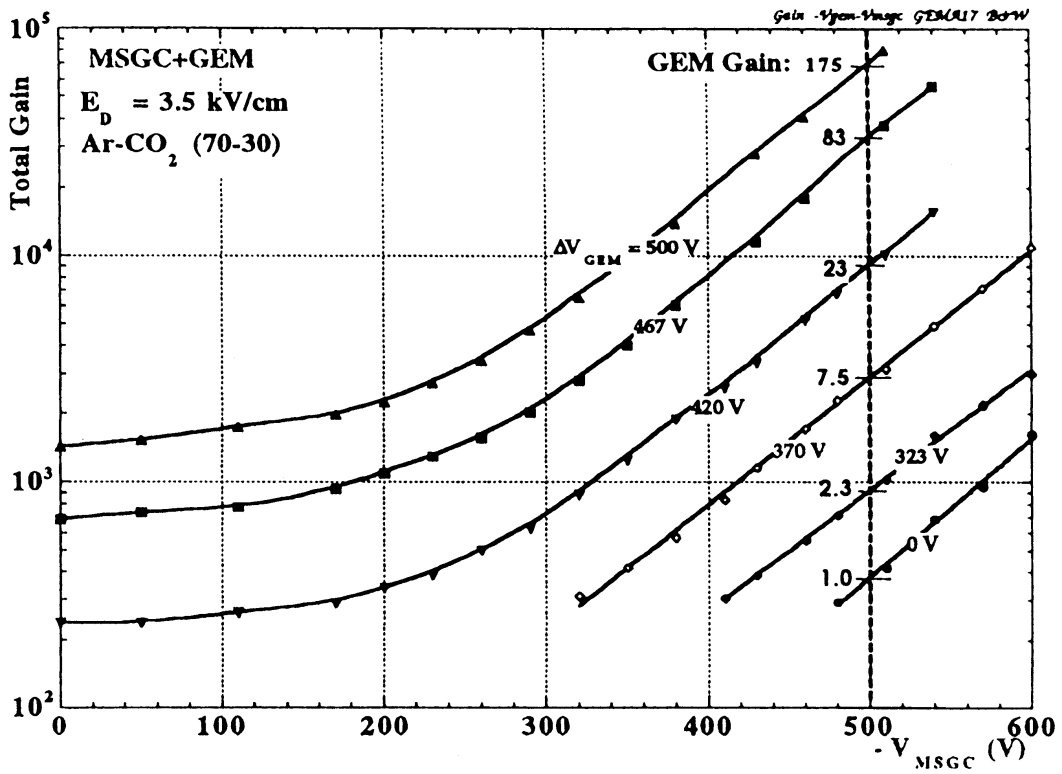
(figs from Hoch, PhD Thesis)

GEM combined with MSGC readout



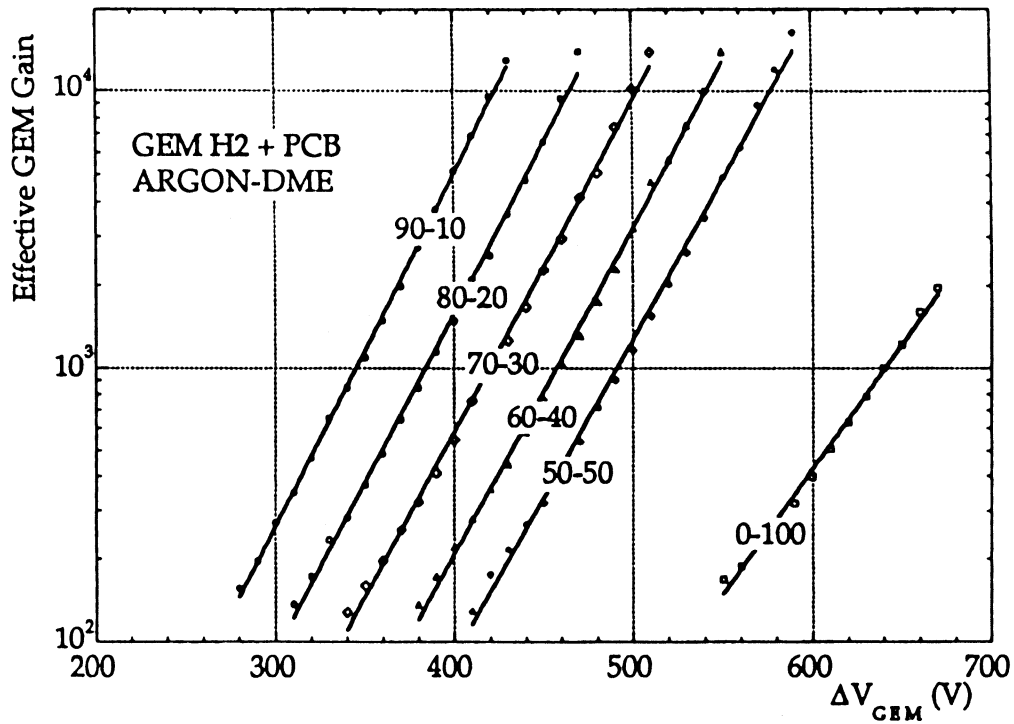
(from Hoch, Kadyk)

Combined gain of GEM + MSGC for various GEM gains



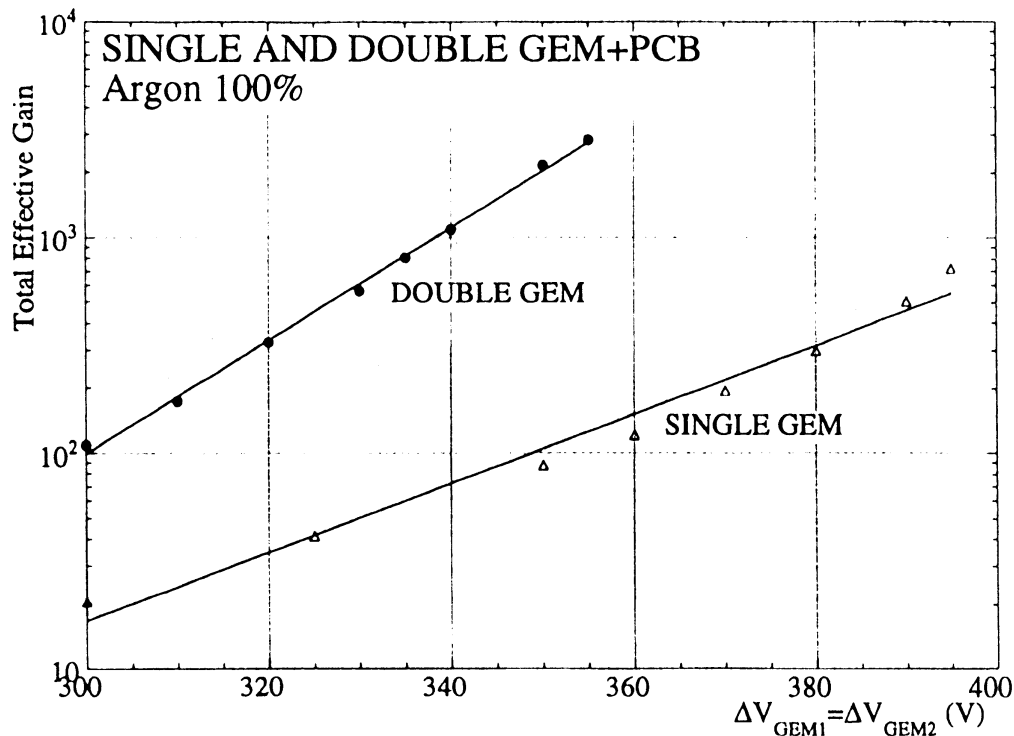
(from Sauli)

Gain of GEM structure alone for various Argon-DME mixtures



(from Sauli)

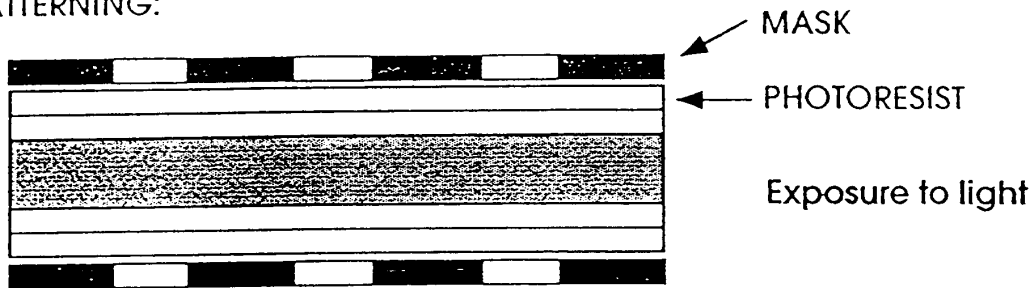
GEMs can be cascaded to obtain higher gain



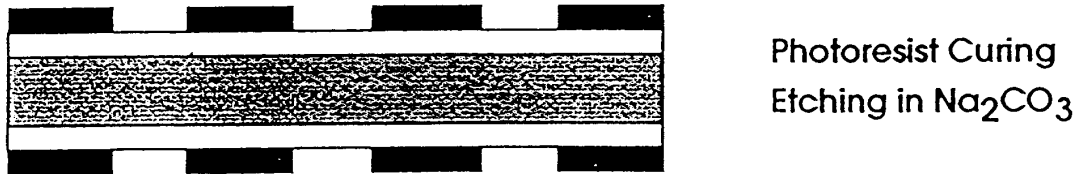
(from Sauli)

GEM fabrication utilizes photolithography and etching

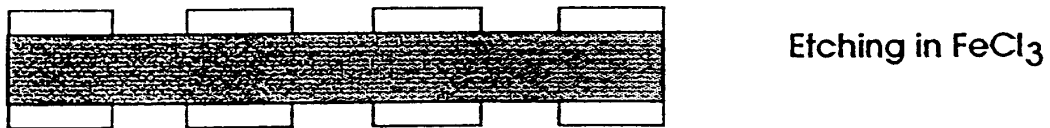
PATTERNING:



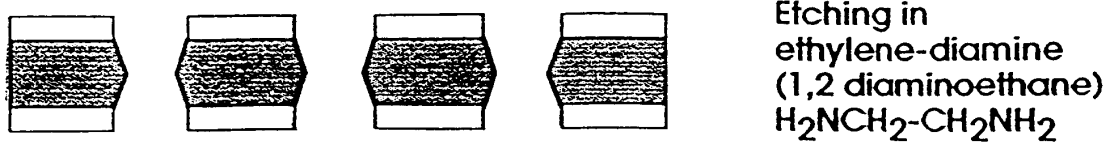
DEVELOPMENT:



METAL ETCHING:

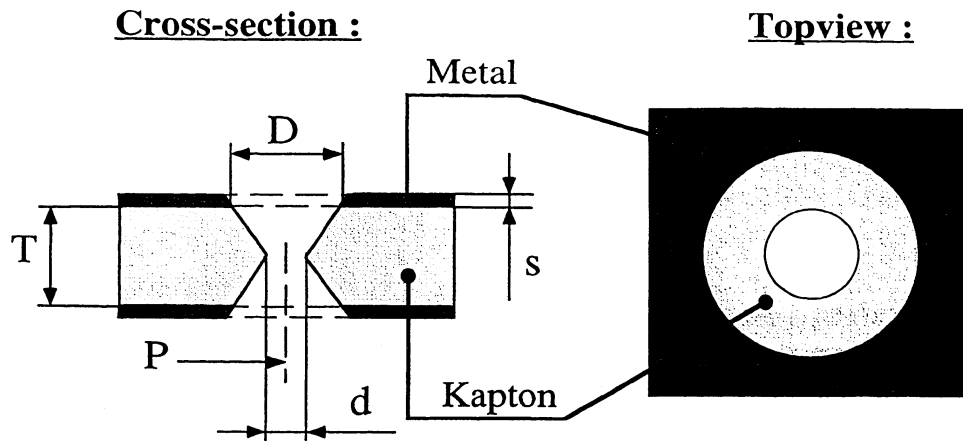


KAPTON ETCHING:



(from Hoch, Kadyk)

Double-sided etching forms a double-conical hole



(from Hoch)

Typical dimensions:

$$T = 50 \mu\text{m}$$

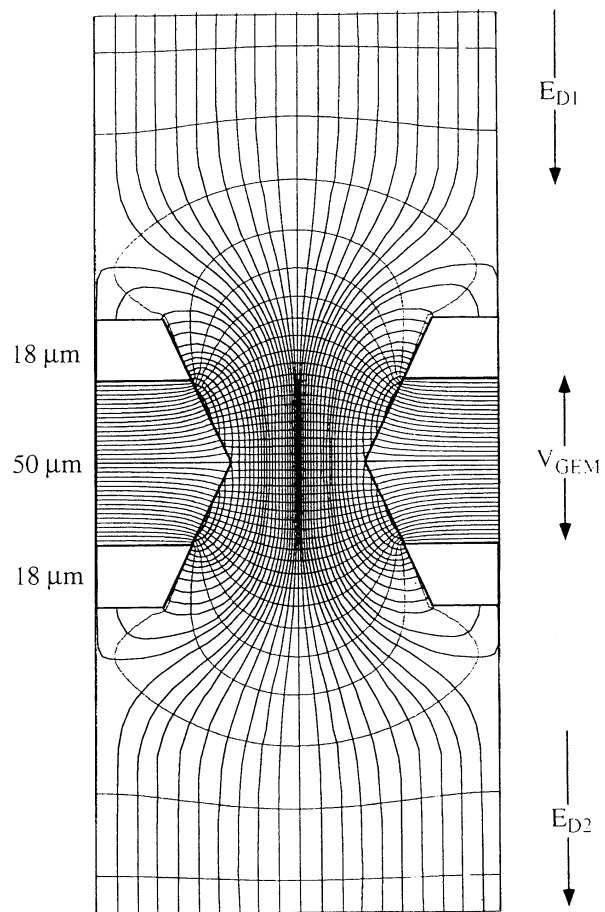
$$s = 5 \mu\text{m}$$

$$D = 100 \mu\text{m}$$

$$d = 60 \mu\text{m}$$

Pitch 150 – 200 μm

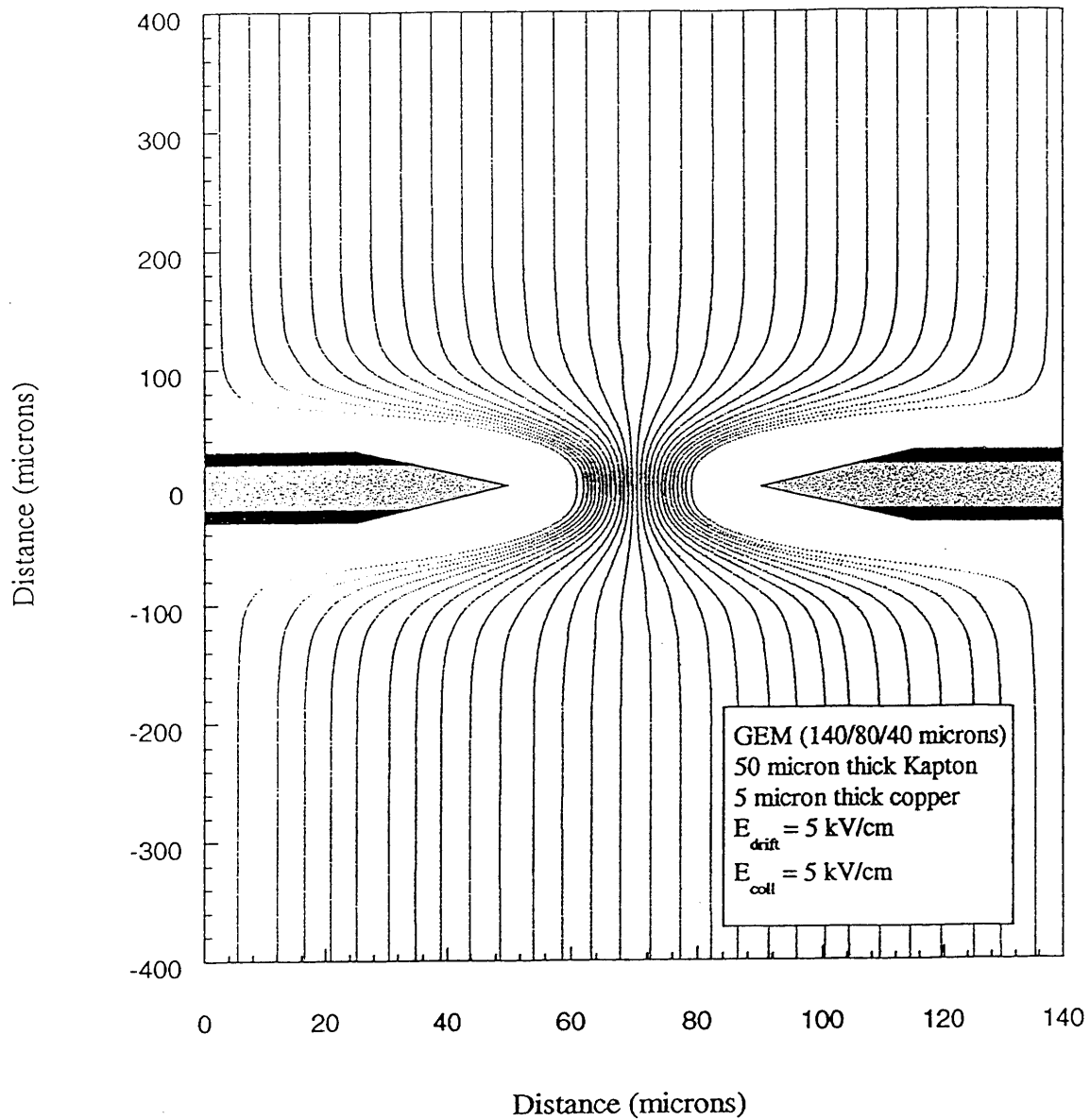
Field distribution



$$V_{\text{GEM}} = 360 \text{ V} \quad E_{\text{D1}} = E_{\text{D2}} = 3 \text{ kV/cm}$$

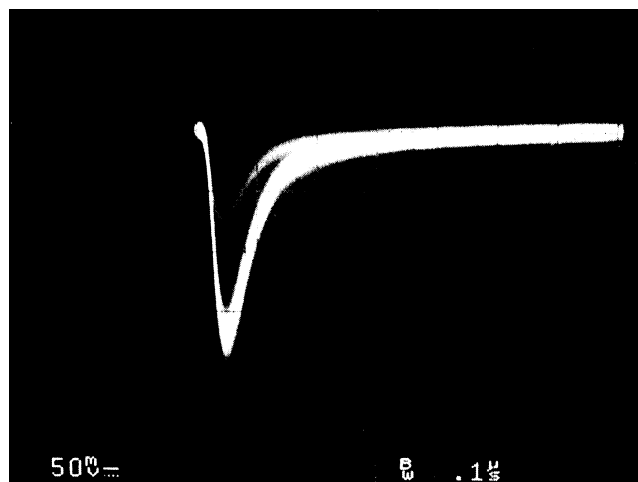
(from Kadyk et al.)

As discussed for Frish grids, the geometry and field distribution can be chosen to provide ~100% transmission for electrons.

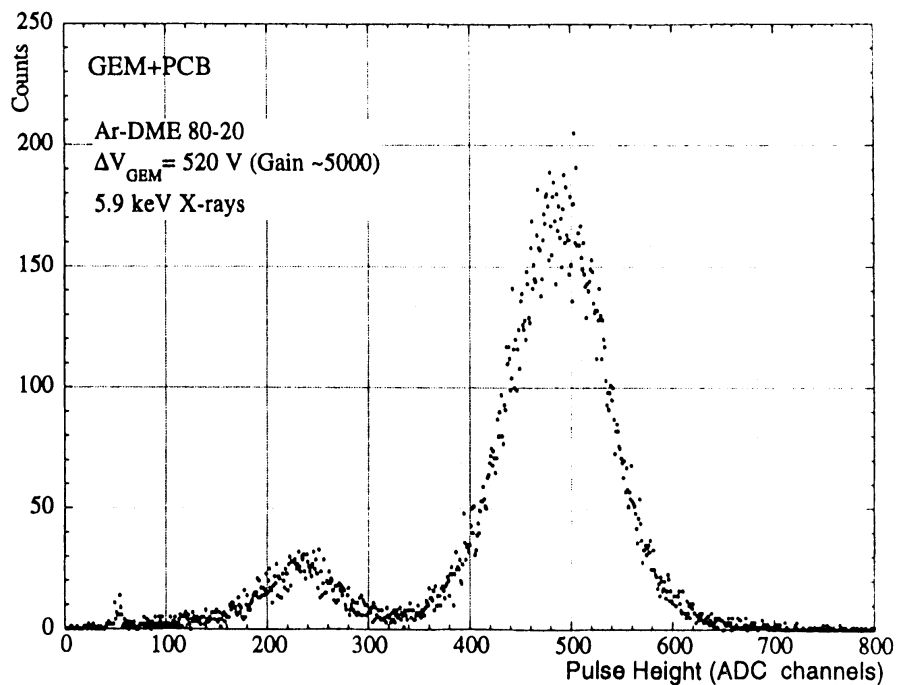


(from Kadyk et al.)

Signal pulses are ~100 ns
in duration



Spectrum taken with ^{55}Fe source



(from Sauli)

Sufficiently high gains are possible with GEMs alone without additional gain in the readout structure (i.e. a simple strip or pixel array can be used instead of an MSGC or MGC).

The GEM separates the gain element from the readout electrode, so the readout electronics are less susceptible to damage by sparking.